Molecular Crystals and Liquid Crystals
Publication details, including instructions for authors and subscription information:
http://www.tandfonline.com/loi/gmcl16

Transverse Electric Field Effect in a Cholestric Liquid Crystal

Young Se Kwon [a]

[a] Department of Electrical Science, Korea Advanced Institute of Science, Seoul, Korea.

Version of record first published: 20 Apr 2011.

To cite this article: Young Se Kwon (1981): Transverse Electric Field Effect in a Cholestric Liquid Crystal, Molecular Crystals and Liquid Crystals, 65:3-4, 227-240

To link to this article: http://dx.doi.org/10.1080/00268948108082136

Mol. Cryst. Liq. Cryst., 1981, Vol. 65, pp. 227–240
0026-8941/81/6504-0227$06.50/0

Printed in the U.S.A.

Transverse Electric Field Effect in a Cholesteric Liquid Crystal

YOUNG SE KWON

Department of Electrical Science, Korea Advanced Institute of Science, Seoul, Korea.

(*Received April 29, 1980*)

The electric field effects of a room-temperature cholesteric liquid crystal have been studied. The cholesteric liquid crystal used is MBBA mixed with a small quantity of cholesteryl nonanoate. When a low frequency (~kHz) AC voltage is applied transversely to the liquid crystal film, grating structures (Williams-Domain-Like Structure and Periodic Distorted Structure) are observed. These structures can be used for the optical modulation of a laser beam.

Several observations of electrohydrodynamic instabilities in nematic liquid crystals under the applications of transverse (parallel to the liquid crystal film) electric field were reported in the literature.[1,2] In this paper the behaviour of a cholesteric liquid crystal film under the applied transverse electric field is discussed.

A CHOLESTERIC WITH NEGATIVE DIELECTRIC ANISOTROPY

The cholesteric liquid crystal used was a mixture of *p*-methoxybenzylidene-*p*-*n*-butylaniline (MBBA) and cholesteryl nonanoate (CN). Silver electrodes with a narrow (~25.4 μm) gap were fabricated on glass plates. The gap was made by vacuum deposition using an aluminum wire (~17.8 μm) as a mask and the typical thickness of the electrodes was ~1000 Å. For these thin electrodes, the transverse electric field is non-uniform for the liquid crystal cells used (6.4–25.4 μm thick).

The top layer and the substrate with electrodes on, were then held at an angle of ~30° to the vapor stream of silicon monoxide inside the vacuum chamber, for homogeneous alignment of liquid crystals. The typical evaporation parameters were as follows: (distance between source and target ~50 cm, current in tungsten boat ~140 ampere, time of evaporation ~1 minute, pre-evaporation chamber pressure $\sim 5 \times 10^{-7}$ Torr). Under the above evaporation conditions, the thickness of silicon monoxide film was much less than 1000 Å.

The deposition of silicon monoxide could be checked in this case by the water-break test. The sample was immersed in high-purity water. The film of draining water revealed clearly the boundary between the silicon-monoxide-coated and the uncoated regions on the surface of the glass. It was also observed that the aligned liquid crystal on the surface of metallic electrodes was quite transparent such that the boundary between silicon-monoxide-coated and uncoated regions could be distinguished clearly because of the different reflections from those regions. For thick ($\gg 1000$ Å) silicon monoxide films, the thickness can be easily estimated simply by looking at the color of the film under sunlight.

a Williams-domain-like structure (WDLS)

The WDLS was observed when the distortion free-energy of the liquid crystal film was not so large without applied electric field. Then the structure could change into an almost-nematic-like structure under the applied electric field. This is illustrated in Figure 2, which shows a relationship between threshold voltages (peak to peak) for the various phases obtained in the sample and the frequency of the applied sinusoidal voltage. It was found that there were two distinct mechanisms for the WDLS. One of these was connected with a generation of disclination lines which was named WDLS–II while the other one was not and it was named WDLS–I.

We know that under the applied electric field (E), the wall effects are effective typically up to a distance ξ, called the coherence length,[3] from the wall where

$$\xi = \frac{(4\pi K/|\Delta\varepsilon|)^{1/2}}{E}.$$

Using the parameters for MBBA, it is found that $\xi \sim 2$ μm. Then we may think that except for the samples whose pitches are larger than $4\xi \sim 8$ μm, the wall effects and the electric field effects are comparable. It was observed that WDLS–I appeared either when the wall effect was dominant or when the conductivity of the liquid crystal was large. WDLS–II was observed when the wall effect was negligible.

In Figure 1, if we apply an electric field along the y-axis the ionic impurities inside the liquid crystal film will begin to drift along the direction of the electric field. But we have both positive and negative ionic impurities so that the currents due to them must have components parallel and antiparallel to the applied electric field. The two currents which flow in opposite directions side by side can alternate either in the z-y plane or x-y plane. It is assumed that WDLS corresponds to the former case.

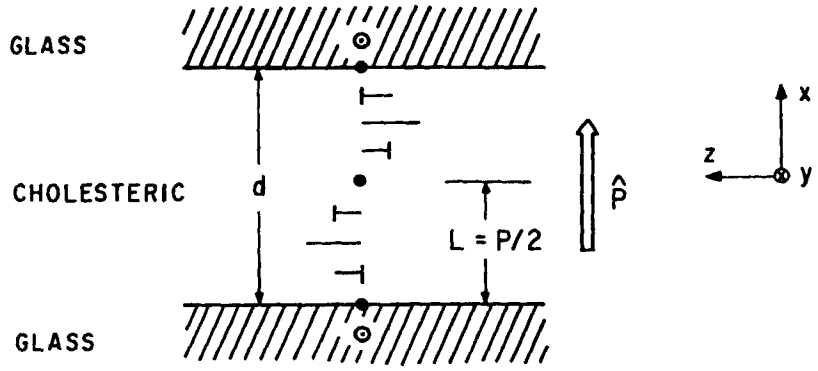

FIGURE 1 The Grandjean planar texture of a cholesteric liquid crystal. The dots inside the glasses denote the directions of the surface alignment. The nails shown indicate the tilted directors in the z-y plane; in the figure a left-handed helix with $d = 2L$ is described. p is the pitch of the cholesteric liquid crystal and $\hat{p}$ is a unit vector along the helical axis.

In liquid crystals, flow of mass is strongly coupled with the alignment of molecules such that the director becomes a strong function of the current. In the case of WDLS the distortion induced by the applied voltage in an otherwise unstressed structure doesn't induce structure transformation and the currents generated by the applied field transfer momentum to the director field such that deformation similar to the Williams domain[4] results. Then we can think of WDLS in a thin slab inside a liquid crystal film as a Williams domain which is complicated because of the fact that the flow direction and the unperturbed director direction can have any angle.

In Figure 3(a), we have a WDLS-I whose threshold behaviour is shown in Figure 2(a). Under crossed polarizers, the planar texture gives the optical extinction of the illuminated light in the microscope. As the applied voltage is increased, the texture shows a birefringence such that the extinct light becomes bright again. As the applied field is further increased it transforms into WDLS-I without storage effects, i.e., WDLS-I returns to the original planar texture when the applied field is turned off. This structure (WDLS-I) has a grating whose periodicity increases as the spacing between electrodes is increased in agreement with the longitudinal nematic case.[5] In Figure 3(b), WDLS-II whose threshold behaviour is given in Figure 2(b), is shown. It will be discussed below in connection with PDS.

b Dynamic scattering mode[6] (DSM)

When the field is increased above a threshold voltage, DSM occurs in all samples and the general threshold behaviour is almost the same for all the samples although the threshold value fluctuates a lot. For low (< 1000 Hz)

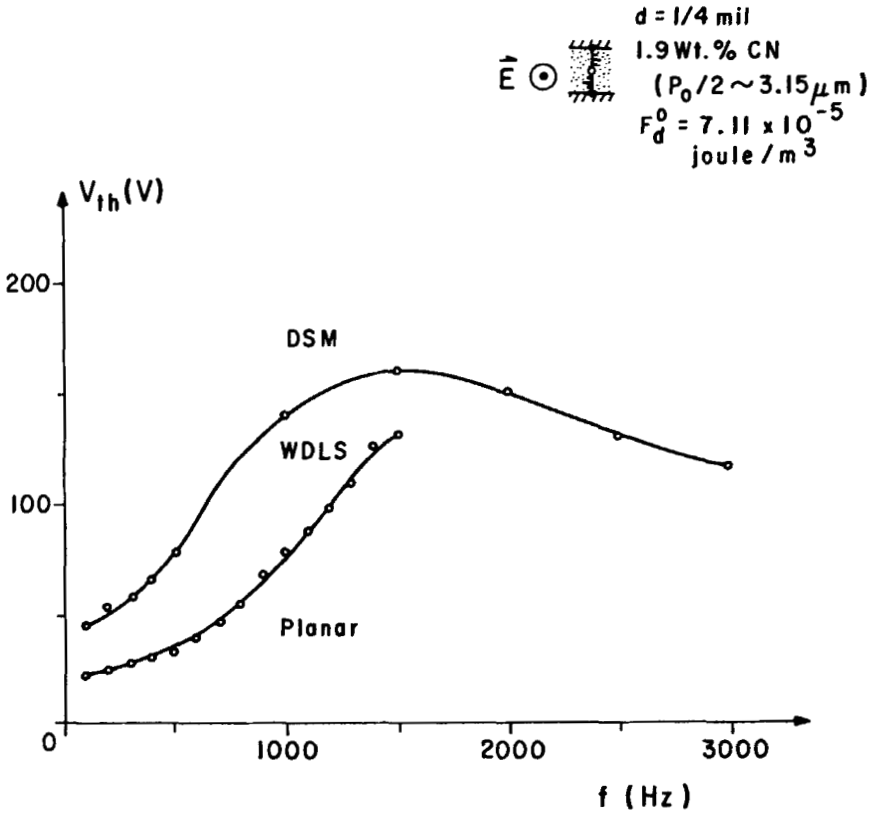

FIGURE 2(a)

FIGURE 2 Relationship between threshold voltages and the frequencies of the applied electric field. F_d^0 is the distortion free-energy density with no applied electric field and p_0 is the free pitch. (a) WDLS-I is obtained for small film thickness and small distortion energy. ($d = 6.4\ \mu m$, $F_d^0 = 7.11 \times 10^{-5}$ joule/m^3, $p_0/2 \sim 3.15\ \mu m$). (b) WDLS-II is obtained for large film thickness and small distortion energy. ($d = 25.4\ \mu m$, $F_d^0 = 4.23 \times 10^{-6}$ joule/m^3, $p_0/2 \sim 12.6\ \mu m$). (c) PDS is obtained for large distortion energy. ($d = 6.4\ \mu m$, $F_d^0 = 4.04 \times 10^{-2}$ joule/m^3, $p_0/2 \sim 2.43\ \mu m$). (d) PDS is not stable when d/p_0 becomes large. ($d = 12.7\ \mu m$, $F_d^0 = 3.44 \times 10^{-3}$ joule/m^3, $p_0/2 \sim 2.43\ \mu m$).

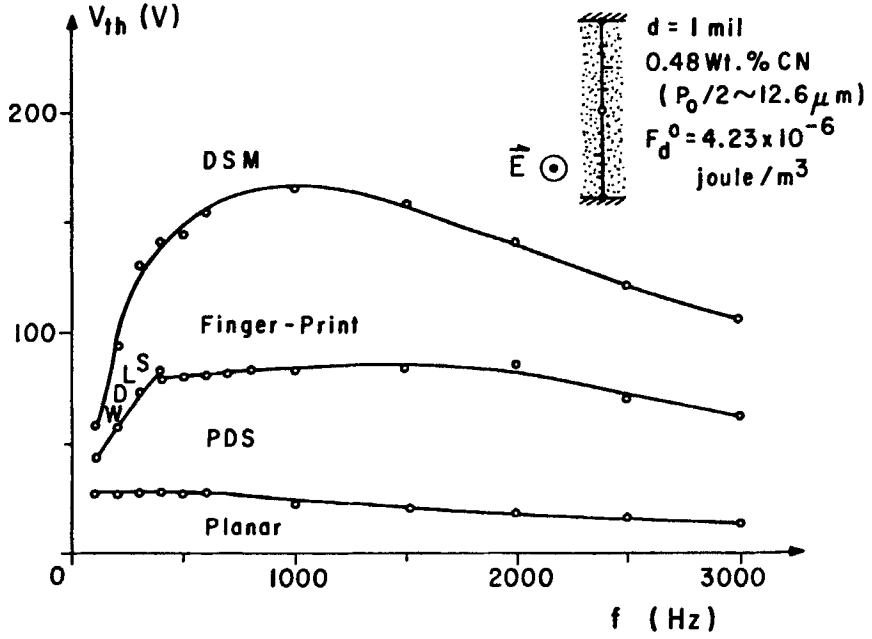

FIGURE 2(b)

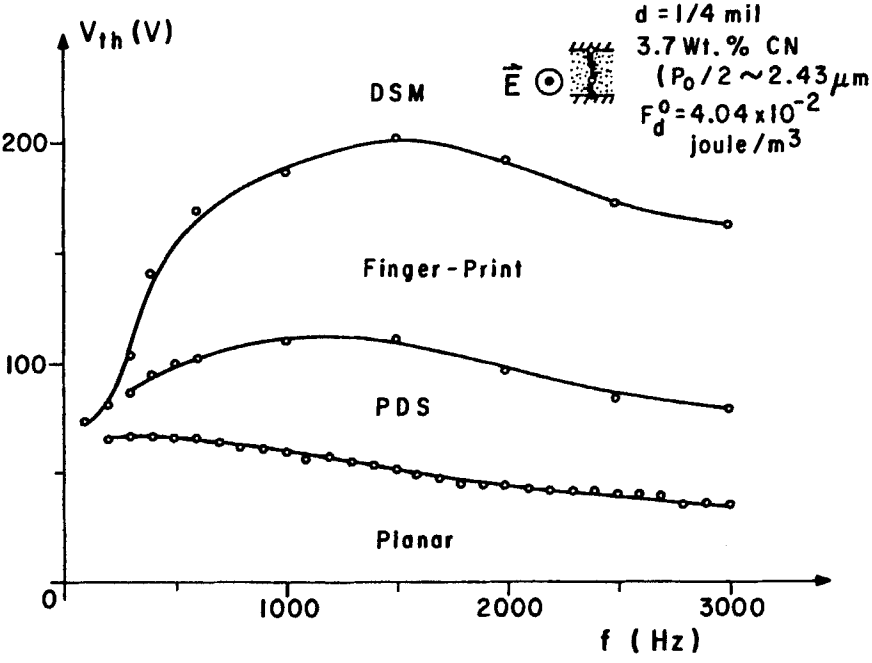

FIGURE 2(c)

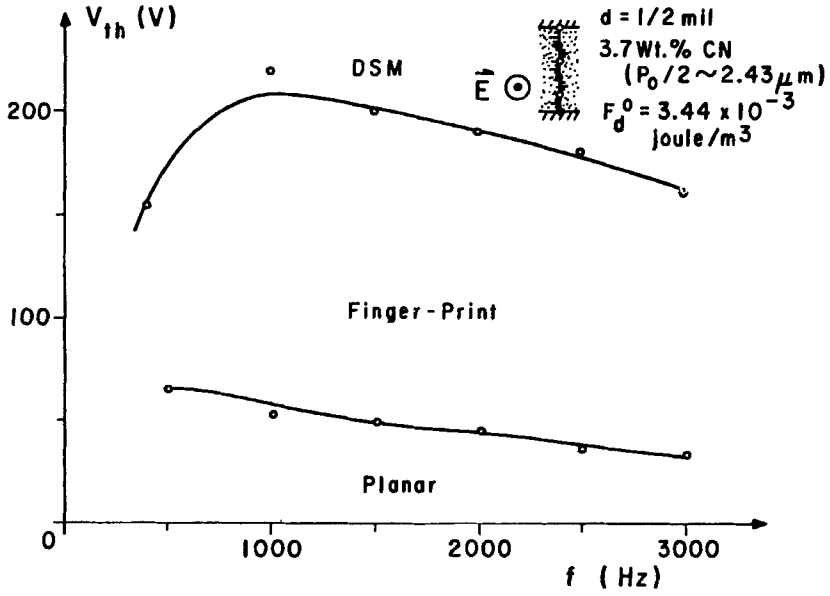

FIGURE 2(d)

frequencies the DSM looks like bundles of quickly moving thread-like flow domains. In high (>1500 Hz) frequencies the scattering domains are small independent swarms which oscillate vigorously. The above behaviour is quite similar to the DSM observed in the corresponding nematic case. For thick (>25.4 μm) samples it seemed that the turbulence was restricted near the boundary wall and the helix structure inside the liquid crystal film was stable. The above phenomena were observed by lowering the focus inside the liquid crystal film in microscope observation.

c PDS and finger-print texture

When the wall effects are strong, the Grandjean planar texture is not easily broken up under the applied electric field. It was observed that when the frequencies of the applied electric field become high (typically above ~1 kHz), the structure goes into a striped texture which we interpret as the Grandjean planar texture undergoing periodic undulation. This structure is similar to the periodic two-dimensional distortion[7] of a cholesteric planar texture observed under an electric field applied normal to a liquid crystal film. Let's call this structure "Periodic Distorted Structure (PDS)."

When the field is increased further in the PDS, the system of disclination lines is developed and the texture turns into the finger-print texture with the

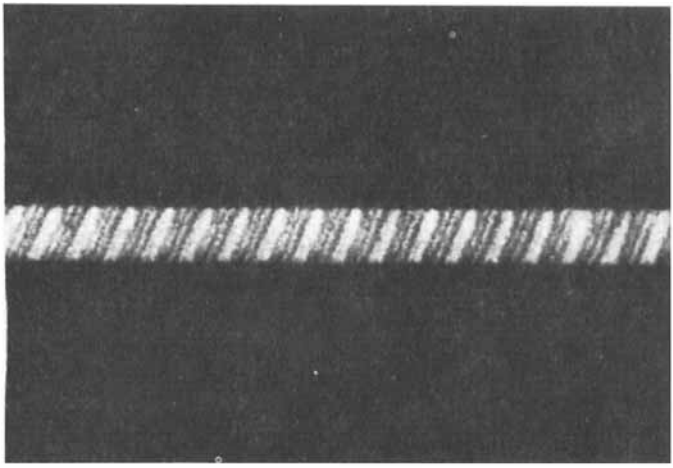

(a)

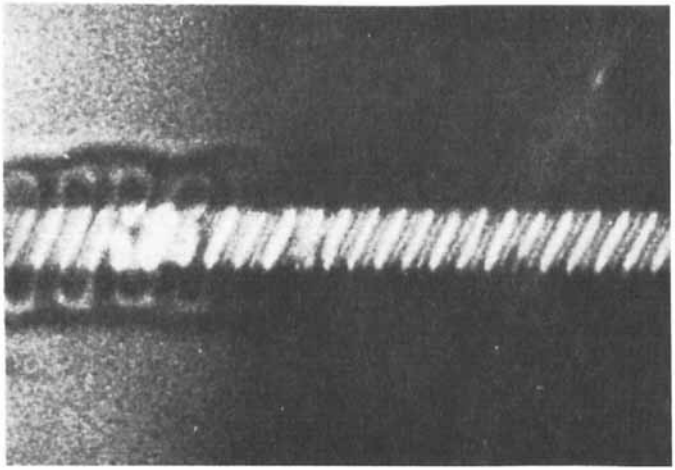

(b)

FIGURE 3 WDLS obtained with low-frequency applied electric field. (a) WDLS-I. (b) WDLS-II.

helix axis along the applied field direction. This picture agrees with the energy consideration, because the cholesteric liquid cyrstal has a negative dielectric anisotropy and the field tries to align the director normal to it in the absence of charge transport. The disclination lines developed are probably nucleated just below the boundary surfaces although they are not necessarily located in the same plane. The disclination line is assumed to be (λ^+, τ^-) type with $m = 1$.[8]

As shown in Figure 2, at low frequencies (below ~ 1 kHz) PDS is usually observed in samples where either the wall effects are negligible, or the distortion occurs mainly due to the direct coupling between the dielectric anisotropy and the electric field, rather than the coupling between the conductance anisotropy and the electric field where the currents induced in the liquid crystal by the applied electric field play a major role. For high frequencies, the charge carriers cannot follow the applied electric field and molecules start to respond to the applied field. The alternation of current distribution is assumed to be in the x-y plane in Figure 1 compared to the case of WDLS where the alternation of currents is in the z-y plane.

In the sample, the electric field inside the liquid crystal film is almost uniform while it is negligible outside the film if the frequency of the applied electric field is much smaller than the inverse of the dielectric relaxation time of the liquid crystal where the dielectric relaxation time is given by

$$\tau_{\text{diel.}} = (\varepsilon_0/\sigma)\varepsilon_r \sim 4 \text{ msec. (MBBA)}$$

In the above ε_0 is the vacuum permittivity while ε_r and σ are the dielectric constant and the conductivity of the liquid crystal respectively. Therefore we notice that even for 200 Hz we cannot neglect the fringing effects. This fringing effect seems very important in the initial formation of PDS which proceeds as follows:

1) When the applied electric field becomes sufficiently large the transparent liquid crystal film forms colored bands adjacent to the electrodes. This color band indicates that the planar texture near the electrodes is deformed due to the strong fringing electric field. The color of the band is green when the analyzer and polarizer are parallel to each other.

2) As the field is increased further, the color band (green) appears at the midpoint between the electrodes in addition to the bands adjacent to the electrodes. This color is so weak and its formation is so gradual that it is hard to notice. Sometimes the bands are disconnected.

3) At a threshold value, the bands change into birefringent periodic structure (PDS). Between the weak green bands there arise strongly colored bands (green-yellow) and the further increase in voltage results in the structure where the green region expands a little at first and the color of the band

changes into a band of multicolor (green to purple). This birefringence seems to represent the onset of an x-component of the director in the structure.

Now, depending on the parameters, the following cases can occur. When either the film is thick or the liquid crystal is under negligible stress, PDS is very unstable at low frequencies. Thus, when the voltage is increased further above the threshold value for PDS the straight line of PDS begins to bend in a curly shape whose amplitude increases as the voltage is increased. The bent line drifts and fluctuates slowly. When the bent line touches both the electrodes, it turns into a disclination line. About the same time, WDLS–II is formed and a portion of it looks like the bent PDS closely packed. On the other hand, the PDS becomes more uniform in other cases. The periodicity in PDS is observed to be reduced as the applied voltages are increased. But at threshold, the formation of PDS is strongly influenced by the fringing effects and the curvature of the deformations of PDS seems not well defined. Figure 4(a) shows a PDS formed between electrodes and in Figure 4(b) the bent PDS mentioned above is shown.

When the field is increased the PDS sometimes transforms into a nematic-like structure instead of finger-print texture. In the nematic-like region the director is in the film and is uniform along the direction normal to the field except at regions very near to the boundary walls. It is separated with a disclination line to the adjacent planar region and observed when the thickness of film is large. Also it is observed that for some samples, as the voltage is

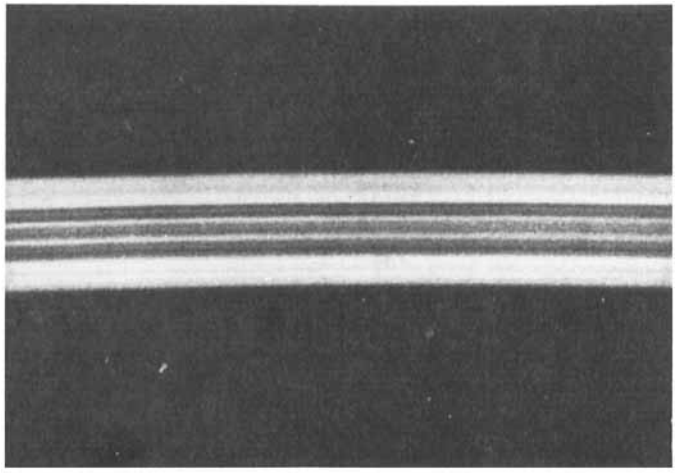

(a)

FIGURE 4 PDS obtained under applied electric field. (a) Uniform PDS obtained for high frequencies of applied voltage. (b) Bent PDS observed below the threshold voltage for WDLS-II.

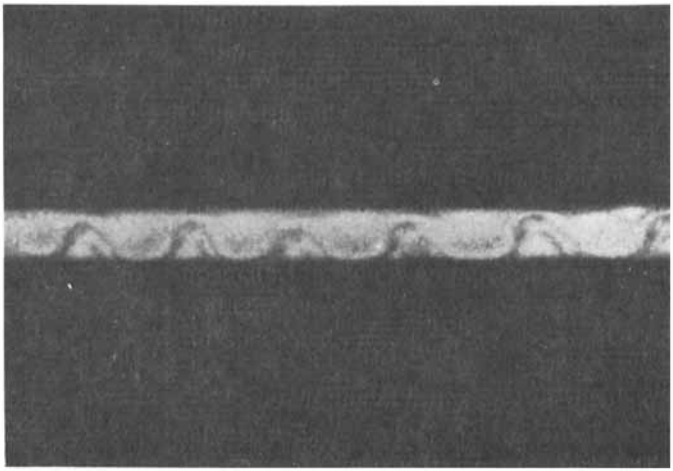

FIGURE 4
(b)

increased, PDS transforms into finger-print texture as soon as PDS is formed, as shown in Figure 2(d). The deformation amplitude in PDS is usually very small. In Figure 2(a), no PDS could be observed under the microscope but diffraction of a HeNe laser beam (6328 Å) indicates its presence at high frequencies.

d Storage modes

Heilmeier and Goldmacher[9] first observed storage effects in a cholesteric liquid crystal film with longitudinal (normal to the liquid crystal film) electric field. In the observation of the transverse electric field effects in a cholesteric liquid crystal film, many structures were found to have quite slow response times (greater than a few seconds). These structures may be important in the application as a storage mode. A few of them are summarized in the following:

1) *Finger-print texture* Matsumoto *et al.*[10] reported that when the surfaces limiting the cholesteric liquid crystal film were treated for homeotropic alignment, the cholesteric adopted the nematic texture with the director normal to the boundary walls by untwisting the helix if the thickness of the film was smaller than the pitch and assumed the finger-print texture otherwise. This is due to the fact that the deformation between a cholesteric helix with $\hat{p}$ parallel to the film and a boundary surface with homeotropic boundary conditions is not strong. But for boundary surfaces treated for

homogeneous alignment the distortion energy between the helix structure of finger-print texture and the wall is large and the finger-print texture obtained under applied electric field relaxes within a few minutes when the field is turned off.

2) *Focal conic to nematic phase transition* For a thick ($d > p$) cholesteric film with homeotropic boundary conditions, it was observed that when an applied voltage exceeded a threshold value, nematic regions with the director normal to the film were nucleated whose sizes were increased as the applied voltage was increased. When the applied voltage was turned off, the structure persisted for a few hours before it returned to the focal-conic texture.

3) *Twin Disclination Lines* When we have $p_0 = 4d$ we notice that we can have $q \equiv 2\pi/p = (1 \pm 1)2\pi/p_0$. In this case a generation of two disclination lines was observed as shown in Figure 5(a) when the applied voltage exceeded a threshold value. Below this threshold value the cholesteric film was in PDS which was bent. It is assumed that the two lines are (τ^-, λ^+) and (λ^+, τ^-) lines with $m = 1$ running together parallel to each other and stuck together on the wall with two disclination points. When the applied voltage was turned off the length of the lines slowly reduced and finally disappeared returning to the original nematic structure ($q = 0$), with a relaxation time of the order of tens of seconds.

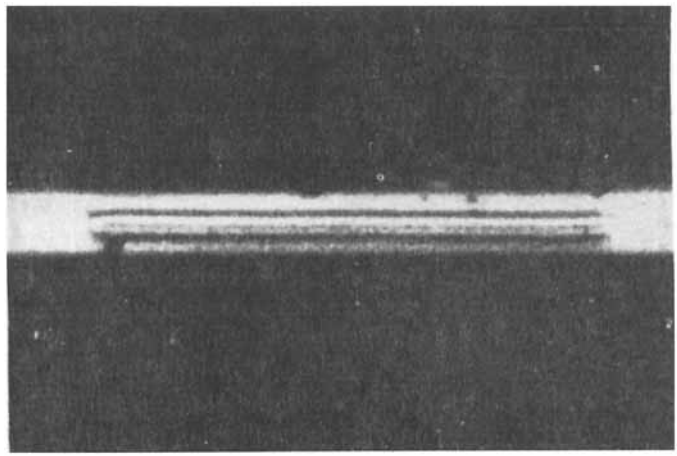

(a)

FIGURE 5 Structures with storage mode. (a) Twin disclination lines. (b) Finger-print texture in a cholesteric with positive dielectric anisotropy.

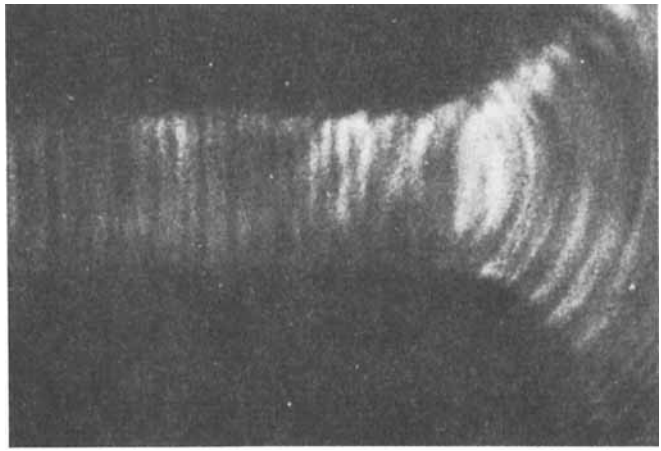

FIGURE 5
(b)

4) *Disclination Loop* For a thick cholesteric film, a nucleation of disclination loops[11] was observed between electrodes when the applied voltage was raised above a threshold value such that WDLS-II was formed. This loop is very stable. Probably the loop was nucleated near the boundary wall. That could be the reason for its stability. When the field was turned off, the loop persisted for a long time (few minutes to few hours).

B Cholesteric with positive dielectric anisotropy

A mixture of CN and "Dymatic Plus" was used for the cholesteric with positive dielectric anisotropy. "Dymatic Plus" is a nematic with positive dielectric anisotropy and was purchased from Vari-Light. First, with the walls treated for homogeneous alignment a planar texture is obtained which begins to untwist its helix as the applied voltage is increased. When the applied voltage is suddenly turned off, a portion of the planar texture exhibits a finger-print texture which dies out within a few seconds. In this case the main mechanism is the dilation of pitch with applied voltage. Second, with the walls treated for homeotropic alignment a transition (focal-conic $\leftrightharpoons$ finger-print $\leftrightharpoons$ nematic) occurs under the applied electric field. For this material with a positive dielectric anisotropy, neither WDLS nor DSM is observed. When the applied field is suddenly turned off, the finger-print texture persists for a few hours. Figure 5(b) shows a finger-print texture under the applied electric field. We observe that $\hat{p}$ is normal to the electric field such that the electric field distribution between the two electrodes is clearly demonstrated.

CONCLUSION

When a low-frequency ac electric field is applied transversely, i.e., along the direction parallel to the liquid crystal film, we obtain (1) voltage-dependent optical rotatory power, (2) grating structures (the Periodic Distorted Structure (PDS) and the Williams-domain-like structure (WDLS)), (3) a fingerprint texture, and (4) a Dynamic Scattering Mode (DSM).

Various electric field effects of liquid crystals have been utilized to modulate or switch the optical guided beam in a liquid crystal optical waveguide[12] with millisecond response times. The various phases mentioned above can be used for the optical modulation when liquid crystals are used either in an integrated optic form or in a bulk form. More studies on the response times are needed for these applications. The storage modes discussed above can be important in the applications as memory devices because of their various relaxation ranges.

In the electric field effects with the electric field applied transversly, the silicon monoxide oblique deposition has been performed such that the director is aligned either parallel or perpendicular to the direction of the applied electric field on the boundary walls. It will be interesting to perform an experiment with the boundary conditions on the director such that the alignments on the walls have a certain angle with the direction of the applied electric field.

Acknowledgment

The author wishes to thank Professor J. R. Whinnery for his helpful suggestions and comments on this work. The work was done at the Electronics Research Laboratory of the University of California, Berkeley, with the support of the National Science Foundation, Grant ENG 73-08077-A03.

References

1. R. Chang, *Mol. Cryst. Liq. Cryst.*, **20** 267 (1973).
2. B. R. Jennings and H. Watanabe, *J. Appl. Phys.*, **47**, 4709 (1976).
3. P. G. de Gennes, *C. R. Acad. Sc. Paris t.*, **266**, 15 (1968).
4. R. Williams, *J. Chem. Phys.*, **39**, 384 (1963).
5. P. A. Penz and G. W. Ford, *Phys. Rev.*, **A6**, 414 (1972).
6. G. H. Heilmeier, L. A. Zanoni, and L. A. Barton, *Proc. IEEE*, **56**, 1162 (1968).
7. H. Arnould-Netillard and F. Rondelez, *Mol. Cryst. Liq. Cryst.*, **26**, 11 (1974).
8. M. Kleman and J. Friedel, *J. Phys. (Paris)*, **30** (Suppl. C4), 43 (1969).
9. G. H. Heilmeier and J. E. Goldmacher, *Proc. IEEE*, **57**, 34 (1969).
10. S. Matsumoto, M. Kawamoto, and N. Kaneko, *Appl. Phys. Lett.*, **27**, 268 (1975).
11. J. Friedel and P. G. de Gennes, *C. R. Acad. Sc. Paris t.*, **268**, 257 (1969).
12. J. R. Whinnery, C. Hu, and Y. S. Kwon, *IEEE J. Quantum Electronics*, **QE-13**, 262 (1977).